Nanoscale Res Lett (2008) 3:386–389
DOI 10.1007/s11671-008-9171-z

NANO EXPRESS

# Controllable Synthesis of Magnesium Oxysulfate Nanowires with Different Morphologies

**X. T. Sun · W. T. Shi · L. Xiang · W. C. Zhu**

Received: 1 September 2008 / Accepted: 8 September 2008 / Published online: 24 September 2008


**Abstract** One-dimensional magnesium oxysulfate $5Mg(OH)_2 \cdot MgSO_4 \cdot 3H_2O$ (abbreviated as 513MOS) with high aspect ratio has attracted much attention because of its distinctive properties from those of the conventional bulk materials. 513MOS nanowires with different morphologies were formed by varying the mixing ways of $MgSO_4 \cdot 7H_2O$ and $NH_4OH$ solutions at room temperature followed by hydrothermal treatment of the slurries at 150 °C for 12 h with or without EDTA. 513MOS nanowires with a length of 20–60 μm and a diameter of 60–300 nm were prepared in the case of double injection (adding $MgSO_4 \cdot 7H_2O$ and $NH_4OH$ solutions simultaneously into water), compared with the 513MOS with a length of 20–30 μm and a diameter of 0.3–1.7 μm in the case of the single injection (adding $MgSO_4 \cdot 7H_2O$ solution into $NH_4OH$ solution). The presence of minor amount of EDTA in the single injection method led to the formation of 513MOS nanowires with a length of 100–200 μm, a diameter of 80–200 nm, and an aspect ratio of up to 1000. The analysis of the experimental results indicated that the hydrothermal solutions with a lower supersaturation were favorable for the preferential growth of 513MOS nanowires along b axis.

**Keywords** Magnesium oxysulfate · Nanowires · Double injection · EDTA · Supersaturation

X. T. Sun · W. T. Shi · L. Xiang (✉) · W. C. Zhu
Department of Chemical Engineering, Tsinghua University, Beijing 10084, China
e-mail: xianglan@mail.tsinghua.edu.cn

X. T. Sun
e-mail: sunxt05@mails.tsinghua.edu.cn

## Introduction

One-dimensional (1D) nanostructured magnesium salts with different morphologies, such as needle [1], rod [2], wire [3], tube [4], and belt [5], have attracted much attention because of their unique properties and potential applications in nanotechnical fields. Up to now much work has been focused on the control of the morphologies of 1D 513MOS since it can be used as the reinforcing agent, the flame retardant, or as the precursor for the fabrication of 1D MgO or $Mg(OH)_2$ [6–8].

It was reported that the 513MOS whisker agglomerates with a length of up to 200 μm and a diameter of 0.8–1.2 μm were formed using $MgSO_4$ and $Mg(OH)_2$ or MgO as the reactants [9, 10]. The sector-like 513MOS whiskers with a length of 20–50 μm and a diameter of 0.2–1.0 μm were synthesized using $MgSO_4$ and NaOH as the raw materials [11–13]. Dispersive 1D 513MOS without agglomerates or the sector-like were formed by employing $MgSO_4$ or the mixture of $MgSO_4$ and $MgCl_2$ as the magnesium source and the weak alkali $NH_4OH$ as the precipitation agent [14–16]. But little work has been reported on the control of the sizes (length and diameter) of the 1D 513MOS and it is still a challenge to synthesize 1D 513MOS with high aspect ratio and perfect uniformity.

Generally the solution with a lower supersaturation was favorable for the anisotropic or 1D growth of the crystals, which can be achieved by using dilute reactants or chelating agents. For example, it was reported that the presence of EDTA can control the morphologies and sizes of the corresponding particles owing to the chelating effects of EDTA with $Ca^{2+}$ [17], $Zn^{2+}$ [18], $Ce^{3+}$ [19], $Fe^{3+}$ [20], $Co^{2+}$ [20], and $Bi^{3+}$ [21], which can change the forms of the aqueous ions, producing a solution with less free metal ions to control the crystals growth. The growth

habits of the crystals can also be altered by the capping effect of EDTA on the surfaces of the crystals.

In the present work the 513 MOS nanowires with high aspect ratio were formed by precipitation of $MgSO_4$ and $NH_4OH$ solutions at room temperature followed by treatment at hydrothermal conditions. The supersaturations of the solutions were controlled at relatively low levels, which were achieved by controlling the mixing ways of the reactants or addition of EDTA. The preferential orientation of 513MOS nanowires was identified and the related process mechanisms were discussed.

## Experimental

### Synthesis of 513MOS Nanowires

Commercial reagents ($NH_4OH$, $MgSO_4 \cdot 7H_2O$, and EDTA) with analytical grade provided by Beijing Chemical Regent Factory were used in the experiments.

Three ways were adapted for the formation of the precursor slurries at room temperature: (1) Single injection: 35 mL of 1.0–1.5 mol $L^{-1}$ $MgSO_4$ was dropped (3.0 mL $min^{-1}$) into 20 mL of 5.0–9.0 mol $L^{-1}$ $NH_4OH$; (2) Double injection: 35 mL of 1.0–1.5 mol $L^{-1}$ $MgSO_4$ and 20 mL 5.0–9.0 mol $L^{-1}$ $NH_4OH$ were dropped (3.0 mL $min^{-1}$) simultaneously into 5–10 mL water; (3) Single injection in the presence of EDTA: 35 mL of 1.0–1.5 mol $L^{-1}$ $MgSO_4$ mixed with varying amount of EDTA was dropped (3.0 mL $min^{-1}$) into 20 mL of 5–9 mol $L^{-1}$ ammonia.

The slurry formed at room temperature was then transferred to a Teflon-lined stainless steel autoclave with an inner volume of 80 $cm^3$, heated (5 °C $min^{-1}$) to 150 °C and kept under isothermal condition for 8.0–12.0 h. The autoclave was cooled down to room temperature naturally after hydrothermal treatment and the product was filtrated, washed, and dried at 105 °C for 12.0 h.

### Analysis

The morphology and the microstructure of the samples were examined with the field emission scanning electron microscopy (FESEM, JSM 7401F, JEOL, Japan), the high-resolution transmission electron microscope (HRTEM, JEM-2010, JEOL, Japan) and the selected area electron diffraction (SAED). The crystallization and the composition of the samples were identified by the powder X-ray diffraction (XRD, D/max2500, Rigaku, Japan) using CuKα ($\lambda = 0.154178$ nm) radiation. The solution pH was detected by Mettler Toledo Delta 320 pH meter. The concentrations of $Mg^{2+}$ and $SO_4^{2-}$ were analyzed by EDTA titration and barium chromate spectrophotometry (Model 722, Xiaoguang, China), respectively.

## Results and Discussion

Figure 1 shows the influence of the preparation ways of the precursors on the morphologies of the hydrothermal products. 1D product with a length of 20–30 μm and an ununiform diameter of 0.3 –1.7 μm were prepared via the single injection route (Fig. 1a). Uniform nanowires with a length to 20–60 μm and a diameter of 60–300 nm were fabricated in the case of the double injection route (Fig. 1b), which may be connected with the decrease of the supersaturation of 513MOS in the solution due to the dilution of the reactants and will be discussed in detail later.

The influence of EDTA on the morphologies of the hydrothermal products was shown in Fig. 2. 1D product with a length of 30–50 μm and a diameter of 0.2–1 μm were formed at $1.0 \times 10^{-3}$ mol $L^{-1}$ EDTA (Fig. 1a). The diameter of the product decreased to 80–200 nm (Fig. 2 b, c) as the EDTA concentration increased up to $1.0 \times 10^{-2}$ mol $L^{-1}$. The clusters of the products were composed of the twisted nanowires with a length of 100–200 μm and an aspect ratio up to 1,000. The diameter of the product was broadened to 0.15–0.6 μm and the length was about 100 μm in the case of $1.0 \times 10^{-1}$ mol $L^{-1}$ EDTA (Fig. 2d).

Figure 3 shows the XRD patterns of the hydrothermal products formed in presence of EDTA. All the diffraction peaks can be indexed as those of the orthorhombic $5Mg(OH)_2 \cdot MgSO_4 \cdot 3H_2O$ (PDF No. 070415). The gradual increase of the diffraction intensities with the increase of EDTA concentration indicated that the presence of EDTA was favorable for the crystallization of 1D 513 MOS. It was also noticed that most of the XRD peaks were attributed to (*h*0*l*) planes, indicating that the 513MOS nanowires may have a preferential growth along b axis owing to its inherent structure.

The HRTEM image and the SAED pattern of the 513MOS nanowires prepared in the presence of

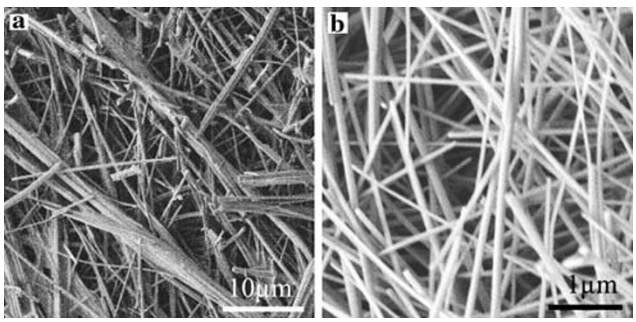


**Fig. 1** The morphologies of the products prepared via single injection (**a**) and double injection (**b**)

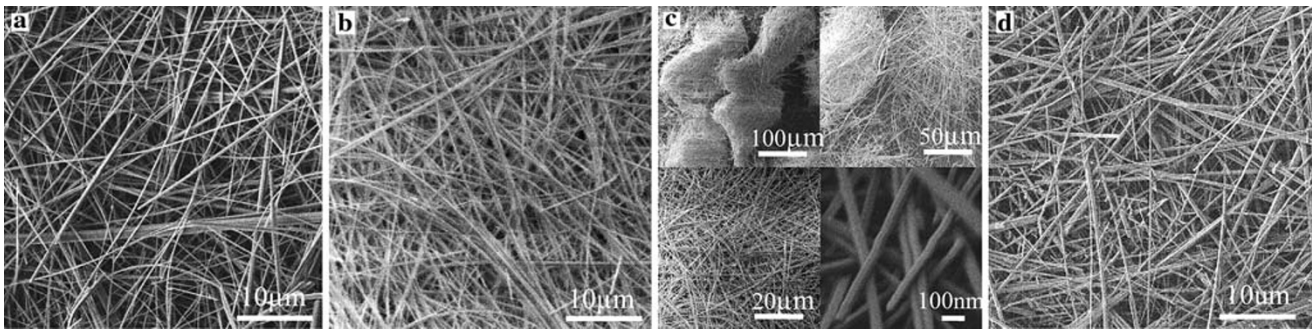


**Fig. 2** Influence of EDTA concentrations on the morphologies of the products (**a**) $1.0 \times 10^{-3}$ mol $L^{-1}$; (**b**, **c**) (different magnifications) $1.0 \times 10^{-2}$ mol $L^{-1}$; (**d**) $1.0 \times 10^{-1}$ mol $L^{-1}$

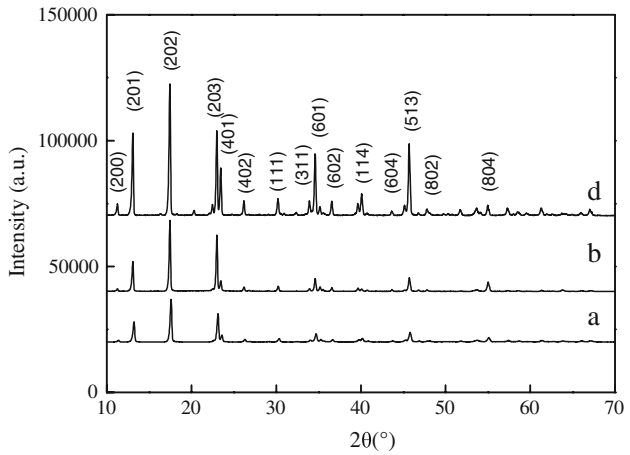


**Fig. 3** XRD patterns of the products shown in Fig. 2

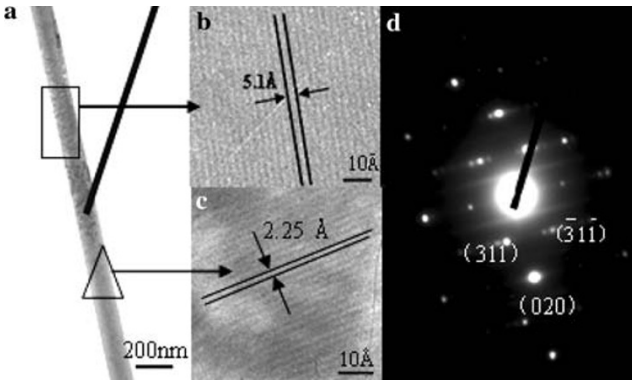


**Fig. 4** TEM (**a**), HRTEM images (**b**, **c**) and SAED pattern (**d**) of 513MOS nanowire

$1.0 \times 10^{-2}$ mol $L^{-1}$ EDTA were shown in Fig. 4. The interplanar distances of the lattice fringes parallel (Fig. 4b, corresponding to the rectangular part of the nanowire in Fig. 4a) and with a 72° angle (Fig. 4c, corresponding to the trigonal part of the nanowire in Fig .4a) to the growth direction of the whiskers were 5.1 and 2.25 Å, quite similar to the spacing of (202) plane (d (202) = 5.12 Å) and (114) plane (d (114) = 2.255 Å), respectively, indicating the preferential orientation of the nanowires along the [010] direction, which was reconfirmed by the SAED analysis in Fig. 4d and also identical with the XRD analysis shown in Fig. 3.

Figure 5 shows the influence of the preparation ways of the $Mg(OH)_2$ precursors on the variation of $[Mg^{2+}]$ and the supersaturation of 513MOS with the hydrothermal time. The supersaturation of 513MOS was presented by $[Mg^{2+}]^6[SO_4^{2-}][OH^-]^{10}$ according to the following formation reaction[13]:

$$6Mg^{2+} + SO_4^{2-} + 10OH^- + 3H_2O = 5Mg(OH)_2 \cdot MgSO_4 \cdot 3H_2O \quad (1)$$

The presence of EDTA led to the decrease of $[Mg^{2+}]$ (Fig. 5a) and the supersaturation of 513MOS (Fig. 5b), which may be connected with the chelating and/or the capping effects of EDTA. EDTA can form stable chelating complexes with $Mg^{2+}$. The slow release of $Mg^{2+}$ from the complexes might be favorable for the 1D growth of 513MOS. The varying binding abilities of EDTA on different planes may also inhibit the radial growth and promote the axial growth of the 513MOS nanowires.

The increase of $[Mg^{2+}]$ and the supersaturation of 513MOS within initial 8 h of reaction should be attributed mainly to the dissolution of the $Mg(OH)_2$ precursor, and the decrease of $[Mg^{2+}]$ and the supersaturation of 513MOS after 6–10 h of reaction may be connected with the formation of 513MOS. The lower supersaturations of 513MOS achieved in either the double injection route or in the presence of minor amount of EDTA were favorable for the formation of 513MOS nanowires with high aspect ratio.

## Conclusion

513MOS nanowires with a length of 20–60 μm and a diameter of 60–300 nm were synthesized via the double injection-hydrothermal reaction and the uniform 513MOS nanowires with a length of 100–200 μm and a diameter of

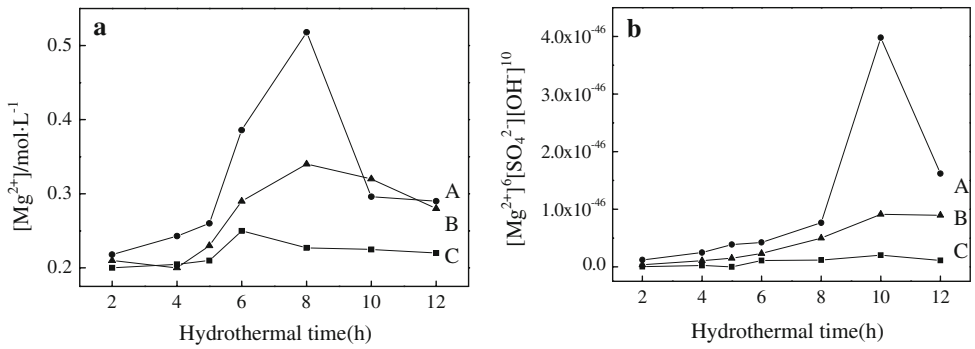


**Fig. 5** Variations of $[Mg^{2+}]$ (**a**) and super-saturation of 513OS (**b**) with hydrothermal time. Preparation ways of $Mg(OH)_2$ precursor: A—single injection without EDTA, B—double injection without EDTA, C—single injection with $1.0 \times 10^{-2}$ mol $L^{-1}$ EDTA

80–200 nm were formed via single injection EDTA-assisted hydrothermal reaction route. The lower supersaturations of 513MOS achieved in either the double injection route or in the presence of minor amount of EDTA, were favorable for the preferential growth of 513MOS along b axis, leading to the formation of 513MOS nanowires with high aspect ratios.

**Acknowledgment** This work is supported by the National Natural Science Foundation of China (No.50574051).

## References

1. Y. Ding, G.T. Zhang, H. Wu, B. Hai, L.B. Wang, Y.T. Qian, Chem. Mater. **13**(2), 435–440 (2001). doi:10.1021/cm000607e
2. J.P. Lv, L.Z. Qiu, B.J. Qu, Nanotechnology **15**(12), 1576–1581 (2004). doi:10.1088/0957-4484/15/11/035
3. Y. Li, Z.Y. Fan, J.G. Lu, R.P.H. Chang, Chem. Mater. **16**, 2152–2154 (2004)
4. W.L. Fan, S.X. Sun, L.P. You, G.X. Cao, X.Y. Song, W.M. Zhang et al., Chem. Mater. **13**, 3062–3065 (2003)
5. Z.Z. Zhou, Q.H. Sun, Z.S. Hu, Y.L. Deng, Phys. Chem. B **110**(27), 13387–13392 (2006). doi:10.1021/jp0612228
6. H.D. Lu, Y. Hu, J.F. Xiao, Z.Z. Wang, J. Mater. Sci. **41**, 363–367 (2006). doi:10.1007/s10853-005-2374-0
7. H.D. Lu, Y. Hu, L. Yang, Z.Z. Wang, Z.Y. Chen, W.C. Fan, Macromol. Mater. Eng. **289**, 984–989 (2004). doi:10.1002/mame.200400165
8. X.T. Sun, L. Xiang, Mater. Chem. Phys. **109**, 381–385 (2008). doi:10.1016/j.matchemphys.2007.12.005
9. P.H. Ma, Z.Q. Wei, G. Xu, J.Q. Bao, X.M. Wen, J. Mater. Sci. Lett. **19**, 257–258 (2000). doi:10.1023/A:1006779229191
10. Z.Q. Wei, H. Qi, P.H. Ma, J.Q. Bao, Inorg. Chem. Commun. **5**, 147–149 (2002). doi:10.1016/S1387-7003(01)00367-7
11. H. Iwanaga, T. Ohyama, K. Reizen, T. Matsunami, J. Ceram. Soc. Jpn. **102**(5), 436–441 (1994)
12. L. Xiang, F. Liu, J. Li, Y. Jin, Mater. Chem. Phys. **87**, 424–429 (2004). doi:10.1016/j.matchemphys.2004.06.021
13. J. Li, L. Xiang, Y. Jin, J. Mater. Sci. **41**, 1345–1348 (2006). doi:10.1007/s10853-006-7339-4
14. Y. Ding, G.T. Zhang, S.Y. Zhang, X.M. Huang, W.C. Yu, Y.T. Qian, Chem. Mater. **12**, 2845–2852 (2000). doi:10.1021/cm000249f
15. X.X. Yan, D.L. Xu, D.F. Xue, Acta Mater. **55**, 5747–5757 (2007). doi:10.1016/j.actamat.2007.06.023
16. D.N. Yang, J. Zhang, R.M. Wang, Z.F. Liu, Nanotechnology **15**, 1625–1627 (2004). doi:10.1088/0957-4484/15/11/043
17. K.J. Westin, A.C. Rasmuson, J. Colloid Interface Sci. **282**, 370–379 (2005). doi:10.1016/j.jcis.2004.09.071
18. K.J. Westin, A.C. Rasmuson, J. Colloid Interface Sci. **282**, 359–369 (2005). doi:10.1016/j.jcis.2004.03.029
19. L. Dileo, D. Romano, L. Schaeffer, B. Gersten, C. Foster, M.C. Gelabert, J. Cryst. Growth **271**, 65–73 (2004). doi:10.1016/j.jcrysgro.2004.07.027
20. F. Luo, C.J. Jia, W. Song, L.P. You, C.H. Yan, Cryst. Growth Des. **5**(1), 137–142 (2005). doi:10.1021/cg049940b
21. D.E. Zhang, X.J. Zhang, X.M. Ni, J.M. Song, H.G. Zheng, J. Magn. Magn. Mater. **305**, 68–70 (2006). doi:10.1016/j.jmmm.2005.11.030